Synchronization of metronomes

James Pantaleone
Department of Physics, University of Alaska, Anchorage, Alaska 99508

Synchronization is a common phenomenon in physical and biological systems. We examine the synchronization of two (and more) metronomes placed on a freely moving base. The small motion of the base couples the pendulums causing synchronization. The synchronization is generally in-phase, with antiphase synchronization occurring only under special conditions. The metronome system provides a mechanical realization of the popular Kuramoto model for synchronization of biological oscillators, and is excellent for classroom demonstrations and an undergraduate physics lab. © *2002 American Association of Physics Teachers.*
[DOI: 10.1119/1.1501118]

I. INTRODUCTION AND SUMMARY

Synchronization is the process where two or more systems interact with each other and come to move together. It is commonly observed to occur between oscillators. Synchronization differs from the well-known phenomena of resonance, where an oscillator responds to an external periodic signal. Collections of oscillators are observed to synchronize in a diverse variety of systems, despite the inevitable differences between the oscillators. Synchronization is a fundamental theme in nonlinear phenomena and is currently a popular topic of research.[1]

Biology abounds with examples of synchronization.[2,3] Populations of certain cicada species emerge simultaneously with periods of 13 or 17 years.[4] Huge swarms of fireflies in South-East Asia gather in the same tree to flash in synchrony (see, for example, Ref. 5). Networks of pacemaker cells in the heart beat together.[6] An example from psychology is the synchronization of clapping in audiences.[7] There are many physical examples also. The voltage oscillations of superconducting Josephson junctions are observed to synchronize.[8,9] Neutrino oscillations in the early universe may also exhibit synchronized oscillations.[10] More generally, synchronized chaotic dynamics has been studied as a promising way of exploiting chaotic systems.[11]

The earliest known scientific discussion of synchronization dates back to 1657 when Christian Huygens built the first pendulum clock.[12] Huygens continued to refine the pendulum clock, trying to develop a reliable timepiece for maritime use in order to solve the longitude problem.[13] To improve reliability and to allow for continued timekeeping while one clock was being serviced, Huygens tried systems of two pendulum clocks mounted on a common base. He observed that the clocks would swing at the same frequency and 180 degrees out of phase. This motion was robust—after a disturbance the synchronized motion came back in about one-half hour.[14]

Surprisingly, it appears that there have been relatively few subsequent attempts at studying the synchronization of pendulums. In 1906 Kortweg[15] studied weakly coupled, small amplitude motion of pendulums, but without any explicit damping or driving in the analysis. Blekhman[16] examined a similar system experimentally and theoretically and found two possible synchronized states; in-phase and antiphase motion, corresponding to phase differences of approximately 0 and 180 degrees. Recently, Bennett *et al.*[14] have re-examined and reproduced Huygens original results.

Here we examine a variant of Huygens' original system, two pendulum metronomes on a light, easily movable platform. For small intrinsic frequency differences, the oscillators generally synchronize with a small phase difference, that is, in-phase. This system makes an excellent classroom demonstration: it can be assembled quickly, synchronization occurs in a few tens of seconds, the mechanical motion is visually appealing, and the metronomes' ticks provide an added indication of the pendulum bob's motion. The system is also useful for an experimental study of synchronization. The audible ticks (and/or the base motion) provide an easy way to quantify the relative motion of the pendulum bobs. The ticks can be recorded and used to study the approach to synchronization and the small phase difference between the synchronized metronomes.

The results are well described by a simple model. The metronomes are described as van der Pol oscillators[17] and the coupling between the metronomes comes from the undamped motion of the base. Using this model, the absence of the antiphase synchronization that Huygens and others observed is readily explained. The large oscillation amplitudes (45 degrees) of the pendulum bobs' motion destabilize the antiphase synchronization. However, antiphase synchronization can be produced in the metronome system by either adding large damping to the base motion, or by going to very large oscillation frequencies.

From the model, approximate evolution equations are derived using the method of averaging. These equations are used to calculate stability diagrams showing the parameter regions where the in-phase and the various possible antiphase synchronization states exist. In a particular, experimentally accessible parameter region, the approximate evolution equations simplify to a single, effective, first-order differential equation that is commonly used in textbook discussions of synchronization. We then consider many metronomes and show that the effective phase evolution equations are equivalent to the Kuramoto model, which is commonly used to describe self-driven, biological oscillators.[18,19] Several possible extensions of the present work are given at the end of this article.

II. METRONOME SYSTEM AND EQUATIONS OF MOTION

Our system consists of two metronomes resting on a light wooden board that sits on two empty soda cans (see Fig. 1). The metronomes are Wittner's Super-Mini-Taktell (Series
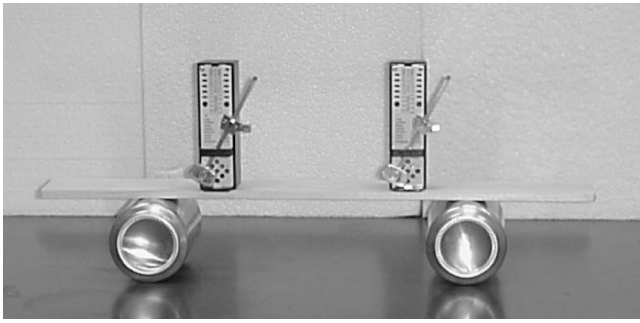
Fig. 1. Picture of two metronomes sitting on a light, wooden board which lies on two empty soda cans.

880), and are claimed to be the world's smallest pendulum metronome (mass 94 g). These metronomes were chosen because they were inexpensive and have a light base. Energy is supplied to each metronome by a hand wound spring. The frequency of the metronome is adjusted by changing the position of a mass on the metronome's pendulum bob. The metronomes' standard settings range from 40 ticks per minute (largo) to 208 ticks per minute (prestissimo), but frequencies outside of this range are possible. For the measurements performed in this paper the highest standard frequency settings were used, which corresponds to 104 oscillations per minute because the metronomes tick twice per cycle. The wooden board on which the metronomes rest is light (58 g), flat with smooth sides, and long enough to support several metronomes. The base supports were empty beverage containers (12 fl. oz). To insure that they rolled smoothly and evenly, they were washed and their pop-tops and a little of the surrounding metal on their ends were removed.

A. The equations of motion

For the equation of motion of a single metronome on a moving base, we use

$$\frac{d^2\theta}{dt^2} + \frac{mr_{c.m.}g}{I}\sin\theta + \epsilon\left[\left(\frac{\theta}{\theta_0}\right)^2 - 1\right]\frac{d\theta}{dt}$$
$$+ \left(\frac{r_{c.m.}m\cos\theta}{I}\right)\frac{d^2x}{dt^2} = 0, \tag{1}$$

where θ is the angle the pendulum makes with the vertical, I is the moment of inertia of the pendulum, m is the mass of the pendulum, $r_{c.m.}$ is the distance of the pendulum's center of mass from the pivot point, g is the acceleration of gravity, and x is the horizontal position of the base. The first two terms in Eq. (1) are the usual ones that describe the motion of a pendulum, that is, the angular acceleration and the gravitational torque. The third term in Eq. (1) crudely models the metronomes' escapement[20] and any damping of the bob's motion from air resistance. This term is of the van der Pol type and increases the angular velocity for $\theta < \theta_0$ and decreases it for $\theta > \theta_0$. For small ϵ, this term will produce stable oscillations with an amplitude of approximately $2\theta_0$ in the isolated oscillator (see, for example, Ref. 21). The last term in Eq. (1) describes the effect of the base motion on the metronome. Because the base moves, the metronome is in a noninertial reference frame and thus experiences an inertial or fictitious force $F_{inertial} = -m\,d^2x/dt^2$ (see, for example,

Ref. 22). The last term is just the torque produced by this inertial force.

The center of mass of the system of two pendulums is given by

$$x_{c.m.} = \frac{Mx + mx_1 + mx_2}{M + 2m}, \tag{2}$$

where M is the mass of the base, and

$$x_i = x + a_i + r_{c.m.}\sin\theta_i \tag{3}$$

denotes the horizontal position of the ith pendulum bob. Here a_i denotes the constant position difference between the ith metronome and the base board. The mass of the soda cans is neglected in Eq. (2). If we neglect all external forces on the system, the equation of motion of the base is contained in

$$\frac{d^2x_{c.m.}}{dt^2} = 0. \tag{4}$$

Equation (4) neglects the damping of the base motion, because the pendulum bob's damping mechanism is contained in the van der Pol term which is not an external force. This approximation appears reasonable because the base motion is smaller and slower than that of a pendulum bob, so the effect of air drag on the base should be relatively unimportant. The only initial conditions considered correspond to the center-of-mass velocity equal to zero. Then $x_{c.m.}$ and the a_i are position constants that are irrelevant to the equations of motion, and can be eliminated by an appropriate choice for the origin of the coordinate system. Thus, the position of the base is given by

$$x = -\frac{m}{M + 2m} r_{c.m.}(\sin\theta_1 + \sin\theta_2), \tag{5}$$

where x, θ_1, and θ_2 are time-dependent variables. Equation (5) describes the coupling between the metronomes. The generalization of Eq. (5) to more than two metronomes is straightforward.

For two metronomes, the coupled system of equations may be written as

$$\frac{d^2\theta_1}{d\tau^2} + (1+\Delta)\sin\theta_1 + \mu\left(\left(\frac{\theta_1}{\theta_0}\right)^2 - 1\right)\frac{d\theta_1}{d\tau}$$
$$- \beta\cos\theta_1\frac{d^2}{d\tau^2}(\sin\theta_1 + \sin\theta_2) = 0, \tag{6a}$$

$$\frac{d^2\theta_2}{d\tau^2} + (1-\Delta)\sin\theta_2 + \mu\left(\left(\frac{\theta_2}{\theta_0}\right)^2 - 1\right)\frac{d\theta_2}{d\tau}$$
$$- \beta\cos\theta_2\frac{d^2}{d\tau^2}(\sin\theta_1 + \sin\theta_2) = 0. \tag{6b}$$

We have changed variables to a dimensionless time variable $\tau = \omega t$, where

$$\omega^2 = \frac{mr_{c.m.}g}{I} \tag{7}$$

is the square of the average angular frequency of the uncoupled, small amplitude oscillator without damping or driving. This frequency differs only slightly from the angular frequency of the uncoupled, nonlinear oscillator, ω_{pen}. The largest correction comes from large oscillation amplitude effects

$$\omega_{\text{pen}} \approx \omega(1 - \tfrac{3}{2}\gamma), \tag{8}$$

where

$$\gamma = \frac{\theta_0^2}{6} \tag{9}$$

parametrizes the leading large angle corrections to pendulum motion $[\sin\theta/\theta_0 \approx \theta/\theta_0 - \gamma(\theta/\theta_0)^3]$. Equation (8) assumes that the steady-state amplitude of the oscillations is approximately twice the angle appearing in the van der Pol term, θ_0. Note that the correction to ω in Eq. (8) from the van der Pol term is of order μ^2 and so is neglected. The relative frequency difference between the oscillators is

$$\Delta \approx \frac{\omega_1 - \omega_2}{\omega}. \tag{10}$$

The dimensionless coupling parameter is

$$\beta = \left(\frac{mr_{\text{c.m.}}}{M + 2m}\right)\left(\frac{r_{\text{c.m.}}m}{I}\right), \tag{11}$$

where the first factor comes from the base motion, Eq. (5), and the second factor from the inertial torque, Eq. (1).

B. System parameters

The dynamics of the system depends on the small, dimensionless parameters γ, Δ, β, and μ. These parameters depend on the average frequency. For all the measurements done here, $\omega_{\text{pen}} = 10.9$ Hz, which corresponds to 208 ticks per minute as obtained from the metronome scale. For this setting the maximum swing amplitude of a single, uncoupled metronome was about 45 degrees, which corresponds to $\theta_0 = 0.39$ rad, which is half the maximum swing angle. Thus, large angle effects enter proportional to the parameter $\gamma = 0.025$ [see Eq. (9)]. The intrinsic frequency difference parameter Δ can be varied by changing the position of the adjustable mass on one of the metronomes. This quantity is most accurately measured by uncoupling the two metronomes, that is, taking them off the base and placing them on the table, and measuring the time interval (with a stopwatch) between when their "ticks" overlap.

The coupling parameter β depends on the physical parameters of the metronome and of the base. It can be decreased by adding mass to the base. Equation (11) for β can be rewritten as

$$\beta = \left(\frac{x_0\omega^2}{g}\right), \tag{12}$$

where

$$x_0 = \frac{mr_{\text{c.m.}}}{M + 2m} \tag{13}$$

is the distance scale of the base motion [see Eq. (5)]. This distance was determined by weighing and measuring parts of the system to obtain

$$x_0 = 0.088 \text{ cm}, \tag{14}$$

$$\beta = 0.011 \tag{15}$$

where β was calculated using $\omega \approx \omega_{\text{pen}}$. These values agree reasonably well with the values obtained by direct measurement of the base motion.
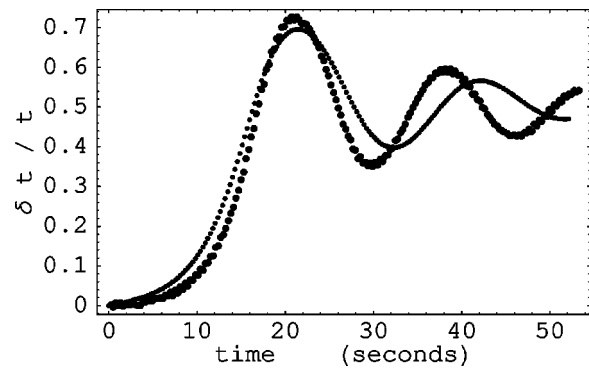

Fig. 2. Plot of the relative time lag versus time. The metronomes' pendulums are started with equal but opposite deflections, and they evolve to synchronized oscillations a half cycle away. The evolution is away from the unstable antiphase oscillations and toward the stable in-phase oscillations. The dark dots are the experimental data and the light dots are a numerical solution of Eq. (6).

The remaining parameter of the system is the van der Pol damping/driving parameter, μ. To determine μ, numerical solutions of Eq. (6) were found using Mathematica. These numerical solutions were compared to the observations and the value $\mu = 0.010$ was chosen to best fit the data in Figs. 2 and 3. The numerical results are included in these figures.

III. EXPERIMENTAL OBSERVATIONS

A. Two metronomes

For small frequency differences, the metronomes were observed to synchronize for all initial conditions where the initial amplitudes were large enough to engage the escapement mechanism. Synchronization was attained on a time scale of order tens of seconds. This phase locked state was maintained until the metronomes springs wound down. For the standard parameters given previously, the synchronized oscillators always had only a small phase difference, that is, they exhibited in-phase synchronization. Synchronization with a phase difference near 180 degrees, antiphase synchronization, was not observed except under altered configurations (see later discussion).

Phase differences between the metronomes can be heard as a very small time difference between the clicks of the
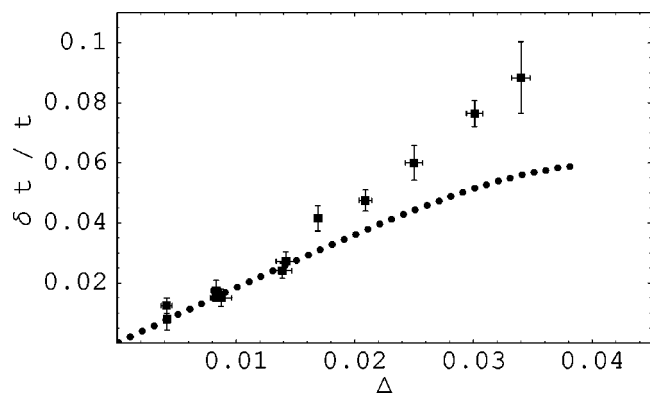

Fig. 3. Plot of the relative time lag versus the intrinsic frequency difference. The results are independent of the initial conditions. The boxes with error bars are the experimental data and the black dots are a numerical solution of Eq. (6).

metronomes. The clicks can easily be recorded using a microphone to provide a record of how the phases evolve. It is possible to do this with a single microphone, but the use of two microphones (one for each metronome) improves the ability to separate the signals. The microphones, data interface, and data analysis software used were all part of PASCO's Science Workshop.[23]

The relaxation to the synchronized state is shown in Fig. 2. The relative time lag between the metronomes (the difference in tick times of the two metronomes divided by the average oscillation period) is plotted as a function of time. The two pendulums were started at rest, approximately 180 degrees out of phase, and with a very small frequency difference ($\Delta \approx 10^{-3}$). Figure 2 shows the system relaxing to the in-phase synchronized state, which is half a cycle away from the initial state. The evolution is initially very slow, with the rate increasing with the separation. This observed behavior indicates that the antiphase state is an unstable fixed point—although it might also be a small bottleneck, that is, close to a saddle node bifurcation. The oscillations around the in-phase state damp out on a time scale of tens of seconds.

After the oscillators have settled down to synchronized motion, small differences in their intrinsic frequency cause a small, steady state phase difference. The fast oscillator leads the slow oscillator by a small amount. The relative time lag between the oscillators as a function of the intrinsic frequency difference is shown in Fig. 3. The relative time lag is approximately the phase difference divided by 2π. As Fig. 3 shows, the time lag increases as the frequency difference increases until a threshold is reached. For frequency differences larger than this threshold, phase locking is not possible. We recorded several time lags at each frequency difference, chosen at random over several minutes. The spread in the time lag was used to generate the error bars shown in Fig. 3. This spread might be due to nonuniformities in the escapement mechanism.

B. Antiphase synchronization

The original observations of Huygens found phase locking in two pendulum clocks with a phase difference close to 180 degrees.[12] This antiphase state was the only type of synchronization observed in a recent reproduction of Huygens experiment using pendulum clocks.[14] However, for the standard metronome system discussed here, the phase locked state always had a phase difference close to zero. Other phase locked states were not observed irrespective of the initial starting configuration of the metronomes. Huygens' system differed from the one considered here in some important ways. First, the clocks had extremely small frequency differences, of order 10^{-4}. Also, they were mounted on a very massive base so that coupling between the clocks, β, was extremely small. One effect of these small parameters for the clock system was that observations were more difficult, and reportedly took of order of one-half hour for the clocks to settle down to the phase locked state; in contrast, the metronomes typically settle down in tens of seconds. More importantly, the small clock parameters make that system sensitive to effects not relevant for the metronomes.

Attempts were made to reproduce the antiphase synchronization observed by Huygens. For example, mass was added to the base (2 kg), reducing the parameter β by a factor of 10. For this configuration, in-phase synchronization was still the only one observed. However, antiphase synchronization was observed at the standard β value of Eq. (15) when the metronome system was placed on a wet surface. The water increased the adhesion of the soda cans to the surface and thus significantly increased the damping of the base motion. In this configuration, phase locking with a phase difference near 180 degrees was consistently reproducible. This result is consistent with the results of Ref. 14 where damping of the base motion is assumed to be the dominant damping in their system. This assumption is very different from that of the standard metronome system studied here, where damping of the base motion is neglected. In our mathematical model, adding damping of the base motion allows phase locked states with a phase difference near 180 degrees. In the limit of large base damping, the antiphase state becomes the dominant fixed point. Quantitative measurements of the phase difference in this configuration were not made.

Antiphase synchronization also was observed when the metronomes operated at average frequencies much higher than the standard setting. With the adjustable pendulum bob mass completely removed, the metronomes would oscillate at approximately 315 ticks per minute. In this configuration, both in-phase and antiphase synchronization was observed. Increasing the frequency corresponds to increasing β [see Eq. (12)] and to decreasing μ, the dimensionless van der Pol parameter.

C. Several metronomes

The behavior of seven metronomes on a common platform was briefly studied. The platform was large enough so that the pendulum bobs did not hit each other. For the same average frequency given in Sec. II B and small frequency differences, in-phase synchronization of seven metronomes was consistently observed. Note that the size of the base motion [see Eqs. (5) and (13)] is roughly independent of the number of metronomes studied because adding metronomes to the system adds mass to both the base and to the pendulum bob.

IV. ANALYTICAL ANALYSIS

The tendency of metronome systems to synchronize can be understood in various ways. First we present a simple, approximate analysis suitable for use in an intermediate classical mechanics class. Then we present a more general analysis.

A. Heuristic analysis

The general tendency of coupled pendulums to synchronize can be understood easily if we study an approximate version of the present system. In particular, let's consider the case of identical ($\Delta \to 0$), small amplitude ($\gamma \to 0$) oscillators. In terms of scaled sum and difference angle variables

$$\delta = \frac{\theta_1 - \theta_2}{2\theta_0}, \tag{16a}$$

$$\sigma = \frac{\theta_1 + \theta_2}{2\theta_0}, \tag{16b}$$

Eq. (6) takes the approximate form

$$\frac{d}{d\tau}\left[\frac{d\delta}{d\tau} + \mu\left(\sigma^2 + \frac{1}{3}\delta^2 - 1\right)\delta\right] + \delta = 0, \tag{17a}$$

$$\frac{d}{d\tau}\left[\frac{d\sigma}{d\tau}+\mu\left(\frac{1}{3}\sigma^2+\delta^2-1\right)\sigma\right]+(1+2\beta)\sigma=0. \quad (17b)$$

It has been assumed that μ and β are small variables of comparable size (see Sec. II B) and only the leading order terms in these parameters are kept. The reason for using the sum and difference variables δ and σ is now apparent—there are no β terms in Eq. (17a) for δ. The β term describes the coupling of the metronomes through the base motion. This motion is identical for the two metronomes, so the coupling cancels out (to leading order) in the evolution of the amplitude difference, δ.

Near the in-phase synchronization state, $\theta_1 \approx \theta_2$ so that $\delta \ll 1$. When this condition holds, the equation of motion for σ decouples and is

$$\frac{d^2\sigma}{d\tau^2}+\mu(\sigma^2-1)\frac{d\sigma}{d\tau}+(1+2\beta)\sigma=0. \quad (18)$$

Equation (18) is just the equation for a simple van der Pol oscillator. The term in Eq. (18) with a coefficient of μ drives the amplitude to 2, for any small value of μ [see Eq. (25)], and the long-term solution is approximately

$$\sigma(\tau)\approx 2\cos((1+\beta)\tau). \quad (19)$$

Using this solution for σ, and working to leading order in δ, Eq. (17a) becomes

$$\frac{d}{d\tau}\left[\frac{d\delta}{d\tau}+\mu(1+2\cos(2(1+\beta)\tau))\delta\right]+\delta=0. \quad (20)$$

The term in Eq. (20) with a coefficient of μ contains two parts, a constant damping part and a part oscillating at roughly twice the natural frequency of δ. The effects of the oscillatory part cancel on average to a good approximation and can be neglected. The approximate solution for δ is then

$$\delta(t)\approx\delta(0)e^{-\mu\tau/2}\cos(\tau+\chi), \quad (21)$$

where χ is an arbitrary phase shift. Thus near the in-phase state, $\delta\rightarrow 0$, and hence in-phase synchronization is stable.

An experimentally observed quantity is the metronomes' ticks as they relax to synchronization (see Fig. 2). The ticks occur when the θ_i's are a multiple of π. If we use the approximate solutions of Eqs. (21) and (19), the small time difference between the two metronomes' ticks near the fixed point is approximately

$$(\tau_2-\tau_1)_n\approx\delta(0)e^{-\mu\tau_n/2}\sin(\chi-\beta\tau_n), \quad (22)$$

where

$$\tau_n=(2n+1)\frac{\pi}{2} \quad (n=0,1,2,...). \quad (23)$$

Equation (22) describes the evolution toward synchronization observed in Fig. 2, damped oscillations with the frequency of oscillations equal to the difference in frequency between the σ and δ oscillations.

It is instructive to repeat the stability analysis of identical, small angle oscillators near the antiphase state. There $\theta_1 \approx -\theta_2$, so $\sigma \ll 1$. Equations (17a) and (17b) are identical under interchange of σ and δ, except for the β term, but the β term just gives a small change in the frequency. Thus, it is not surprising that near the antiphase state a similar analysis is possible. Then δ evolution decouples to a simple van der Pol oscillator, and σ oscillations damp out to zero. For coupled, identical, *small amplitude* metronomes, the antiphase state is also stable (in agreement with Ref. 16).

Antiphase synchronization was observed experimentally for the metronome system at the standard frequency setting when damping of the base motion was added by wetting the table. Because the base motion is the same for both metronomes, base damping will enter like the β terms do in Eq. (17). Thus base damping will add damping primarily to the evolution of σ and not to δ. Enhanced base damping will stabilize the σ evolution, leading to $\sigma\rightarrow 0$, which corresponds to antiphase synchronization. In Huygens' observations only the antiphase synchronized state was observed. This is apparently because the base damping was much larger than the damping associated directly with the pendulum bobs' motion.

To describe the metronome system in Fig. 1, the previous, simple analysis must be modified to include large amplitude effects ($\gamma\neq 0$) as is done in the following.

B. Method of averaging

The evolution of the angles θ_1 and θ_2 in Eq. (6) is predominantly oscillatory. As zeroth order solutions we take

$$\theta_1=A\theta_0\cos(\tau+\phi), \quad (24a)$$

$$\theta_2=B\theta_0\cos(\tau+\xi), \quad (24b)$$

which are the solutions for the uncoupled, small angle oscillators, that is, when the parameters μ, β, Δ, and γ vanish. When these parameters are nonvanishing but small, A, B, ϕ, and ξ are slowly evolving functions of time. To find this slow time dependence, we use a method called "two-timing" or "the method of averaging" (see, for example, Ref. 21). This perturbative method is designed to avoid secular terms, and thus yields an approximate solution that models the true solution for all time. To leading order in the small variables, the relevant evolution equations are

$$\frac{d\psi}{d\tau}=\frac{1}{8}\left[-3\gamma(A^2-B^2)+8\Delta+4\beta\left\{\frac{B}{A}-\frac{A}{B}\right\}\cos\psi\right], \quad (25a)$$

$$\frac{dA}{d\tau}=\frac{1}{8}[\mu A(4-A^2)+4\beta B\sin\psi], \quad (25b)$$

$$\frac{dB}{d\tau}=\frac{1}{8}[\mu B(4-B^2)-4\beta A\sin\psi]. \quad (25c)$$

Here $\psi=\phi-\xi$ is the phase difference between the oscillators. Equations (25) will be used to find the long term behavior of the system.

The implication of Eq. (25) is straightforward in the limit of a very massive base, $\beta=0$. Then the amplitude evolution equations, Eqs. (25b) and (25c), decouple, and it is apparent that the van der Pol term drives the individual oscillation amplitudes A and B to 2 (as mentioned earlier). If we substitute these amplitude fixed points into the evolution equation for ψ, Eq. (25a), we see that in the long time limit, the phase difference of the uncoupled oscillators simply evolves at a constant rate equal to the frequency difference, Δ. There is no synchronization for uncoupled oscillators.

In general, the implications of Eq. (25) can be analyzed in a similar manner by using a slightly different parametrization. We define the variables r and s as

$$r = \frac{A^2 + B^2}{4}, \tag{26a}$$

$$s = \left| \frac{B}{A} - \frac{A}{B} \right|. \tag{26b}$$

Then Eq. (25) can be rewritten as

$$\frac{dr}{d\tau} = \mu r \left[1 - \left(\frac{s^2 + 2}{s^2 + 4} \right) r \right], \tag{27a}$$

$$\frac{ds}{d\tau} = -\frac{1}{2} [\mu s r + \beta (s^2 + 4) \sin \psi], \tag{27b}$$

$$\frac{d\psi}{d\tau} = \frac{1}{2} \left[\left(\frac{3\gamma r}{\sqrt{s^2 + 4}} + \beta \cos \psi \right) s + 2\Delta \right]. \tag{27c}$$

These equations may be analyzed stepwise to find when synchronization occurs.

In particular, the evolution of r is straightforward. Its qualitative behavior can be easily discerned from a sketch of $dr/d\tau$ versus r. Because both the r and the s dependent term in Eq. (27a) are non-negative, r is monotonically driven to the attractive fixed point r^*,

$$r \to r^* = \frac{s^2 + 4}{s^2 + 2} \tag{28}$$

for any nonzero initial value of r. We substitute this value into Eq. (27b), and then study its fixed point structure. If we set $ds/d\tau = 0$, we find two finite fixed points. A graphical analysis shows that one is attractive and one repulsive. The attractive fixed point is

$$s \to s^* = \frac{\mu}{2\beta \sin \psi} [-1 + \sqrt{1 - 2(2\beta \sin \psi/\mu)^2}], \tag{29}$$

where $-\sqrt{2} \leqslant s^* \leqslant \sqrt{2}$. This attractive fixed point exists except for values of $\beta \sin \psi/\mu$ such that the square root in Eq. (29) becomes imaginary. These fixed point values for s and r may now be substituted into Eq. (27c) to yield a single, effective evolution equation

$$\frac{d\psi}{d\tau} = \frac{1}{2} \left[\left\{ 3\gamma \frac{\sqrt{s^{*2} + 4}}{s^{*2} + 2} + \beta \cos \psi \right\} s^* + 2\Delta \right]. \tag{30}$$

Equation (30) describes the fixed point structure of the phase difference.

For the standard parameters of the system used here ($\beta = 0.011$, $\mu = 0.010$, and $\gamma = 0.025$), Eq. (30) may be simplified further. As Fig. 3 shows, the in-phase, fixed point phase difference is small for small Δ, so we make the approximation that $\sin \psi$ is small. For $2(2\beta \sin \psi/\mu)^2 \ll 1$, Eq. (29) gives

$$s^* \approx -\frac{2\beta}{\mu} \sin \psi, \tag{31}$$

and to leading order in this approximation, the evolution equation for ψ is

$$\frac{d\psi}{d\tau} \approx \left[\Delta - (3\gamma + \beta) \frac{\beta}{\mu} \sin \psi \right]. \tag{32}$$
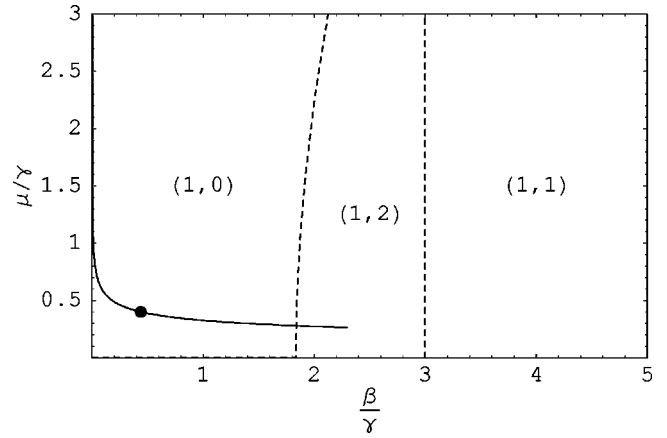
Fig. 4. Stability diagram for identical oscillators ($\Delta = 0$). The regions separated by dashed lines correspond to different values of (n_i, n_a), where n_i and n_a are the number of in-phase and antiphase fixed points, respectively. The large dot shows the parameters for the metronome system studied in this paper; the solid curve estimates how these parameter change for different average frequencies.

Equation (32) has a very simple form and is a standard example in textbooks on nonlinear dynamics (see, for example, Ref. 21). It arises in many branches of science and engineering, and has been used to describe firefly flashing rhythms,[2] the human sleep–wake cycle, Josephson junctions,[8,9] and many other synchronization phenomena. The attractive fixed point gives an approximate expression for the phase difference

$$\psi \to \psi^* \approx \arcsin \left(\frac{\mu \Delta}{\beta (3\gamma + \beta)} \right). \tag{33}$$

An analysis of Eq. (30) shows that Eq. (33) is accurate up to terms of order Δ^3. At larger values of Δ, the phase ψ becomes large and the approximation in Eq. (31) breaks down. The results in Eq. (33) can be compared to Fig. 3 where the relative time lag (which is approximately the phase difference divided by 2π), is plotted as a function of Δ. At small Δ, the slope in Fig. 3 agrees with Eq. (33). At large Δ, the threshold value of ψ, where synchronization is no longer possible, agrees with the value where s^* becomes imaginary.

In addition to varying the frequency difference, the average frequency and the mass of the platform may also be varied. Thus a wide range of Δ, μ, β parameter space is experimentally accessible. For different parameters, different types of fixed points are possible. To map out the possibilities, Eq. (30) was used to find (n_i, n_a), which are the number of attractive in-phase ($\cos \psi > 0$) and antiphase ($\cos \psi < 0$) fixed points, respectively. The types of attractive fixed points that exist for different system parameters are given in Figs. 4 and 5.

The stability diagram for identical oscillators ($\Delta = 0$) is shown in Fig. 4. The dot shows the standard parameters used. It lies in the region $(1,0)$, where only in-phase synchronization occurs, in agreement with experimental observations. The dotted lines indicate the boundaries between different stability regions. For identical oscillators, in-phase synchronization is always possible; however, antiphase synchronization(s) is also possible at larger values of β/γ. When more than one stable fixed point exists, the initial conditions determine which is realized. Although there is only one type of in-phase fixed point, there are two different types of an-
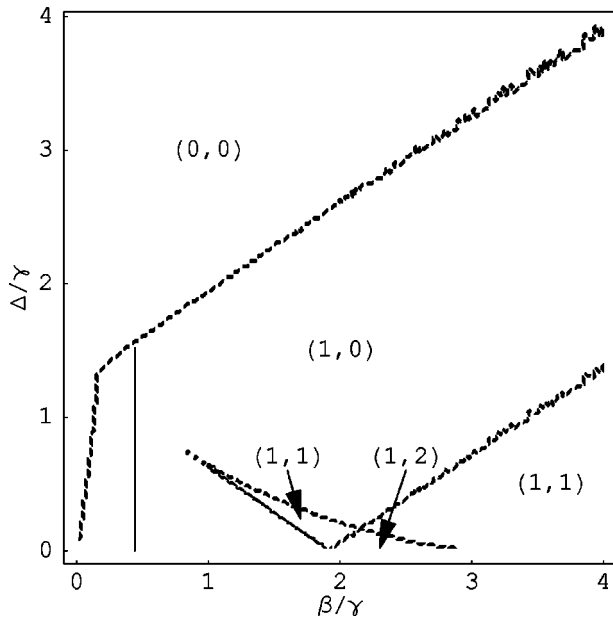
Fig. 5. Stability diagram for nonidentical oscillators. It is assumed that $\mu = 0.011$. The regions separated by dashed lines correspond to different values of (n_i, n_a), where n_i and n_a are the number of inphase and antiphase fixed points, respectively. The solid curve corresponds to the range of frequency differences where synchronization occurred in Fig. 3.

tiphase fixed points. At intermediate values of β/γ, the antiphase fixed point corresponds to where the factor in curly brackets in Eq. (30) vanishes. This factor is a function of $(\sin\psi)^2$, and because it is symmetrical about $\psi = \pi$, there are two attractive fixed points at nonzero values of $\sin\psi$. The left boundary of this region corresponds to where s^{*2} has its maximum value $s^{*2} = 2$. The right boundary of this region corresponds to where s^{*2} has its minimum value $s^{*2} = 0$. For large β/γ, there is only one antiphase fixed point corresponding to $s^* = 0 = \sin\psi$, $\psi = \pi$. This result agrees with the results of the heuristic analysis where it was found that small γ (small amplitude oscillations) corresponds to a (1,1) region.

The solid curve going through the dot in Fig. 4 shows a rough estimate of how the parameters may be varied experimentally by changing the average metronome frequency ($\beta \propto \omega^4$, $\mu \propto 1/\omega$). There is agreement between this phase diagram and the experimental observation of both antiphase and in-phase synchronization when the metronomes were adjusted to unusually high frequencies.

The stability diagram for nonidentical oscillators is shown in Fig. 5. Here μ is taken to have its standard value of $\mu/\gamma = 0.40$. For large values of Δ/γ, no synchronization occurs. As Δ/γ decreases, the first synchronization to occur is in-phase. The boundary separating the (0,0) and (1,0) regions is described approximately by $s = -\sqrt{2}$ for large β/γ and by $\sin\psi = 1$ for small β/γ. The boundary separating the (1,0) region from where antiphase synchronization occurs is more complicated. At vanishing Δ/γ, we note that Fig. 5 agrees with Fig. 4; in particular, there are two stable antiphase states at intermediate values of β/γ, and the boundary point between the (1,0) and (1,2) regions occurs at $s^{*2} = 2$. At nonzero values of Δ/γ, the $s^* \leftrightarrow -s^*$ symmetry is broken, and the boundary splits into two curves that correspond approximately to $s^* = \sqrt{2}$ for the left curve and $s^* = -\sqrt{2}$ for the right. The right curve becomes the main boundary between

the (1,0) and (1,1) regions at larger values of Δ/γ and β/γ. The boundary between the (1,2) and right (1,1) region is different from the boundaries previously described, in that it is not a bifurcation associated with an extremal value of s^*, $\sin\psi$, or $\cos\psi$. It is associated with a saddle node bifurcation intrinsic to Eq. (30).

The solid vertical line in Fig. 5 shows the parameters where synchronization occurs in Fig. 3, $\beta/\gamma = 0.44$ and $0 \leq \Delta/\gamma \leq 1.5$. There is good agreement between the threshold values in Figs. 3 and 5. The region above this curve, where no synchronization occurs, can easily be explored experimentally by further increasing the frequency difference of the metronomes. By changing the average frequency of the metronomes, the parameter regions to the left and right of the solid curve in Fig. 5 also can be explored. (However, a small change in μ/γ would also occur.) In particular, as shown in Fig. 4, values of $\beta/\gamma > 2$ are easily achievable. Thus all the different antiphase states shown in Fig. 5 should be accessible to experimental study.

C. Several metronomes

The previous analysis may be generalized to the case of several metronomes on a common base. Following Eq. (24), the angular position of the ith metronome's pendulum is parametrized as $\theta_i = A_i \theta_0 \cos(\tau + \phi_i)$, where A_i and ϕ_i are slowly varying functions of time. By using the method of averaging, we obtain the evolution equations

$$\frac{dA_i}{d\tau} = \mu\left(\frac{A_i}{2}\right)\left\{1 - \left(\frac{A_i}{2}\right)^2\right\} + \frac{\tilde{\beta}}{N}\sum_{j=1}^{N}\left(\frac{A_j}{2}\right)\sin[\phi_i - \phi_j], \tag{34a}$$

$$\frac{d\phi_i}{d\tau} = \frac{\Delta_i}{2} - \frac{3}{2}\gamma\left(\frac{A_i}{2}\right)^2 + \frac{\tilde{\beta}}{2N}\sum_{j=1}^{N}\left(\frac{A_j}{A_i}\right)\cos[\phi_i - \phi_j], \tag{34b}$$

where N is the number of metronomes, Δ_i parametrizes the frequency differences, $\omega_i^2 \approx 1 + \Delta_i$, and $\tilde{\beta}$ is a generalized version of Eq. (11). If we neglect the mass of the supporting board and two cans compared to the total mass of all the metronomes, we find

$$\tilde{\beta} = \left(\frac{m}{\mathcal{M}}\right)\left(\frac{r_{\text{c.m.}}^2 m}{I}\right), \tag{35}$$

where $\mathcal{M}$ is the mass of a single metronome, and the other parameters represent the same quantities as in Sec. II. Equation (34) describes the evolution of A_i and ϕ_i to first order in small parameters Δ_i, γ, μ, and $\tilde{\beta}$.

Equation (34) may be combined to obtain a simplified expression analogous to Eq. (32). In particular, we consider the limit of small $\tilde{\beta}$, specifically $(\tilde{\beta}/\mu, \tilde{\beta}/\gamma) \ll 1$. This parameter region is where in-phase synchronization is the only attractive final state. It corresponds approximately to the standard parameters described in Sec. II B; however, these limits are better achieved as the average metronome frequency is lowered. In this limit the amplitudes, A_i, have their attractive fixed point close to 2, and the approximate phase evolution equations can be written as

$$\frac{d\phi_i}{d\tau} = -\frac{3}{2}\gamma + \frac{\Delta_i}{2} - \sqrt{\left(3\frac{\widetilde{\beta}}{\mu}\right)^2 + \left(\frac{\widetilde{\beta}}{\gamma}\right)^2}\left(\frac{\gamma}{2N}\right)$$
$$\times \sum_{j=1}^{N} \sin[\phi_i - \phi_j - \xi], \tag{36}$$

where

$$\tan\xi = \frac{\mu}{3\gamma}. \tag{37}$$

This system of equations is a version of the Kuramoto model,[18,19] which was proposed to describe coupled, biological oscillators. The model has been studied extensively in the literature (see, for example, Refs. 2, 3, 24, and 25, and references therein). In general, the system exhibits a phase transition from incoherent oscillations to collective synchronization as the coupling parameter is increased relative to the spread in frequencies. Thus the metronome system provides a simple, mechanical realization of the Kuramoto model.

In discussions of the Kuramoto model, the evolution equations are often presented in a slightly different form. We introduce the order parameter

$$R\, e^{i\psi} = \frac{1}{N}\sum_{j=1}^{N} e^{i\phi_j}, \tag{38}$$

and write the evolution equations as

$$\frac{d\phi_i}{d\tau} = -\frac{3}{2}\gamma + \frac{\Delta_i}{2} - \sqrt{\left(3\frac{\widetilde{\beta}}{\mu}\right)^2 + \left(\frac{\widetilde{\beta}}{\gamma}\right)^2}\left(\frac{\gamma}{2}\right)$$
$$\times R\sin[\phi_i - \psi - \xi]. \tag{39}$$

It is apparent that this model is a mean-field theory where the individual oscillators interact with the average of the other oscillators. For the metronome system this average is provided by the base motion

$$x = -\frac{m}{\mathcal{M}}r_{\text{c.m.}}R\sin\psi, \tag{40}$$

which is the generalization of Eq. (5) to several oscillators. Hence, measurements of the base motion directly yield the order parameter of the system.

At extremely low average frequencies, it is estimated that μ/γ will become large (see Fig. 4). Thus it might be possible to reach the situation where $\xi \approx \pi/2$. In this limit, Eq. (36) implies that the metronomes couple via a cosine-like interaction. This situation is very similar to the description of neutrino oscillations in the early universe.[10] In this limit collective synchronization has neutral stability, that is, it can exist at large coupling parameters, but does not spontaneously occur. It is intriguing that the metronome system might be able to provide a mechanical realization of neutrino oscillations in the early universe. However, this limit is probably quite sensitive to higher order corrections.

V. DISCUSSION

The results in this paper are not a complete investigation of the metronome system. There are many additional avenues that remain to be explored. Some of the obvious ones are given below.

Additional experimental measurements at other parameter values. The parameters that can easily be varied are the av-

erage frequency, the frequency difference, and the base mass, which is analogous to changing μ, Δ, and β, respectively. At higher frequencies, in-phase and a rich structure of antiphase synchronization states can be explored (see Figs. 4 and 5). In particular, the transition regions near the onset of new types of synchronization should be especially interesting.

Measurement of the base motion. Measuring the position of the base would provide a useful continuous order parameter describing the degree of synchronization of the oscillators. For in-phase synchronization, the magnitude of the base motion is a couple of millimeters [see Eq. (13)]. This motion is observable with a typical ultrasonic motion sensor, but is at the lower limits of its resolution. More precise measurements are desirable.

Measurement of the multimetronome system. As more metronomes are added to the system, more opportunities for interesting physics exist. One possibility would be to study the system when it provides a mechanical realization of the Kuramoto model, as discussed in Sec. IV C. In particular, the phase transition that occurs in the Kuramoto model could be observed by measuring the steady-state base motion for different base masses.

Extension of model. The model is in good qualitative agreement with the data. The quantitative agreement would be improved by introducing additional parameters into the model. The present model is economical in that it uses the van der Pol term to describe damping and driving. Quantitative improvement could be obtained by using a more detailed description of the metronome's escapement mechanism plus a damping term for the pendulum bob's motion.

Basins of attraction. At higher average frequencies, several synchronization states occur. The final synchronization state of the system depends on the initial conditions. Each synchronization state should have separate basins of attraction, which could be calculated numerically from the present model and/or studied experimentally.

Unsynchronized motion. The effective evolution equations, Eq. (25), suggest that the unsynchronized motion is quasiperiodic. This behavior could be tested experimentally by using the observed tick times to reconstruct attractors through time-delay plots. In addition, the behavior of a system near a saddle node "bottleneck" could be observed.

Additional base damping. Damping of the base motion could be added to the system in various ways. As noted, this damping enhances the stability of some antiphase synchronization states, thus producing results similar to those found by Huygens.[12] This modified system could be studied experimentally and theoretically.

In addition to the above straightforward generalizations of the present work, several other unlikely but intriguing possibilities exist.

Search for oscillator death. The stopping of oscillations by one or both of the metronomes was observed only at or near when a metronome's spring wound down. However, oscillator death has been observed in the recent study of coupled pendulums clocks,[14] and it might exist for some version of the metronome system.

Search for synchronization when frequencies are a rational ratio. There are many different physical examples of synchronization when the frequencies are near a ratio of integers, for example, the 3/2 ratio between the orbital and rotation periods of the planet Mercury. This type of synchronization was not observed for the present metronome system, in agreement with the result of an averaging analysis,[26]

which found that the metronomes decouple from each other to leading order in small parameters. However it might be possible to enhance this type of synchronization by modifying the basic metronome system.

ACKNOWLEDGMENTS

[1] R. C. Hilborn and N. B. Tufillaro, ''Resource Letter: ND-1: Nonlinear dynamics,'' Am. J. Phys. **65**, 822–834 (1997).

[2] H. H. Strogatz and I. Stewart, ''Coupled oscillators and biological synchronization,'' Sci. Am. **269**, 102–109 (1993).

[3] S. H. Strogatz, ''Norbert Wiener's brain waves,'' Lect. Notes Biomath. **100**, 122–138 (1994).

[4] See J. Cooley and D. Marshall, ''Periodical cicada Page,'' University of Michigan Museum of Zoology, http://www.ummz.lsa.umich.edu/magicicada/Periodical/; F. C. Hoppenstedt and J. B. Keller, ''Synchronization of periodical cicada emergences,'' Science **194**, 335–337 (1976).

[5] D. Attenborough, ''The Trials of Life: Talking to Strangers'' (BBC-TV, 1991), available from Turner Home Entertainment.

[6] D. C. Michaels, E. P. Matyas, and J. Jalife, ''Mechanisms of sinoatrial pacemaker synchronization: A new hypothesis,'' Circ. Res. **61**, 704–714 (1987).

[7] Z. Neda, E. Ravasz, Y. Brechet, T. Vicsek, and A.-L. Barabasi, ''Self-organizing processes: The sound of many hands clapping,'' Nature (London) **403**, 849–850 (2000).

[8] K. Wiesenfeld, P. Colet, and S. H. Strogatz, ''Synchronization transitions in a disordered Josephson series array,'' Phys. Rev. Lett. **76**, 404–407 (1996).

[9] T. Heath and K. Wiesenfeld, ''Mutual entrainment of two nonlinear oscillators,'' Am. J. Phys. **66**, 860–866 (1998).

[10] V. A. Kostelecky, J. Pantaleone, and S. Samuel, ''Neutrino oscillation in the early universe,'' Phys. Lett. B **315**, 46–50 (1993); J. Pantaleone, ''Stability of incoherence in an isotropic gas of oscillating neutrinos,'' Phys. Rev. D **58**, 073002-1–073002-14 (1998).

[11] L. M. Pecora and T. L. Carroll, ''Synchronization in chaotic systems,'' Phys. Rev. Lett. **64**, 821–824 (1990); A. S. Pikovsky, ''On the interaction of strange attractors,'' Z. Phys. B: Condens. Matter **55**, 149–154 (1984);

M. G. Rosenblum, A. S. Pikovsky, and J. Kurths, ''Phase synchronization of chaotic oscillators,'' Phys. Rev. Lett. **76**, 1804–1807 (1996).

[12] C. Hugenii, *Horoloquim Oscilatorium* (Apud F. Muguet, Paris, France, 1673); English translation, *The Pendulum Clock* (Iowa State University Press, Ames, Iowa, 1986).

[13] Navigation at sea was extremely difficult for many centuries until reliable clocks were developed in the late 1700s. See, for example, D. Sobel, *Longitude* (Walker and Co., New York, 1995).

[14] B. Bennett, M. F. Schatz, H. Rockwood, and K. Wisenfeld, ''Huygens' clocks,'' Proc. R. Soc. London, Ser. A **458**, 563–579 (2002).

[15] D. J. Kortweg, ''Les Horloges Sympathiques de Huygens'' (Archives Neerlandaises, Serie II. Tome XI, Martinus Nijhoff, The Hague, 1906), pp. 273–295.

[16] I. I. Blekhman, *Synchronization in Science and Technology* (ASME, New York, 1988).

[17] B. van der Pol, ''Forced oscillators in a circuit with non-linear resistance,'' Philos. Mag. **3**, 64–80 (1927).

[18] A. T. Winfree, ''Biological rhythms and the behavior of populations of coupled oscillators,'' J. Theor. Biol. **16**, 15–42 (1967).

[19] Y. Kuramoto, *Chemical Oscillations, Waves and Turbulence* (Springer, Berlin, 1984).

[20] The escapement controls the speed and regularity of the pendulum. It transfers the energy stored in the spring to the motion of the pendulum by means of wheels, gears, and ratchets.

[21] S. H. Strogatz, *Nonlinear Dynamics and Chaos* (Perseus Publishing, Cambridge, 1994).

[22] G. R. Fowles, *Analytical Mechanics* (Holt Rinehart and Winston, New York, 1977).

[23] PASCO Scientific, http://www.pasco.com/

[24] Y. Kuramoto and J. Nishikawa, ''Statistical macrodynamics of large dynamical systems,'' J. Stat. Phys. **49**, 569–605 (1987); S. H. Strogatz and R. E. Mirollo, ''Stability of incoherence in a population of coupled oscillators,'' *ibid.* **63**, 613–635 (1991); L. L. Bonilla, J. C. Neu, and R. Spigler, ''Nonlinear stability of incoherence and collective synchronization in a population of coupled oscillators,'' *ibid.* **67**, 313–330 (1992); H. Daido, ''Generic scaling at the onset of macroscopic mutual entrainment in limit-cycle oscillators with uniform all-to-all coupling,'' Phys. Rev. Lett. **73**, 760–763 (1994); J. D. Crawford, ''Amplitude expansion for instabilities in populations of globally-coupled oscillators,'' J. Stat. Phys. **74**, 1047–1084 (1994).

[25] S. H. Strogatz, ''From Kuramoto to Crawford: Exploring the onset of synchronization in populations of coupled oscillators,'' Physica D **143**, 1–20 (2000).

[26] J. Pantaleone (unpublished).